A microcalorimetry study on the adsorption of asphaltenes and asphaltene model compounds at the liquid/solid surface.

Diego Pradilla*, Sreedhar Subramanian, Sébastien Simon, Johan Sjöblom.

Ugelstad Laboratory, Department of Chemical Engineering, Norwegian University of Science and Technology (NTNU), NO-7491 Trondheim, Norway.

Isabelle Beurroies, Renaud Denoyel.

Aix Marseille Université, CNRS, MADIREL UMR 7246, 13397 Marseille cedex 20, France.

*Corresponding Author

E-mail: diego.c.p.ragua@ntnu.no
Phone: +47 735 94 080

Notes

The authors declare no competing financial interest.

Abstract

Adsorption of an acidic polyaromatic asphaltene model compound (C5PeC11) and indigenous C_6-asphaltenes onto the liquid-solid surface is studied. The model compound C5PeC11 exhibits a similar type of adsorption with a plateau adsorbed amount as C_6-asphaltenes onto three surfaces (silica, calcite and stainless steel). The model compound BisAC11, with aliphatic end-groups and no acidic functionality, does not adsorb at the liquid-silica surface indicating the importance of polar interactions on adsorption. The values of the adsorption enthalpy characterized by the parameter ΔH_z (the enthalpy at zero coverage) indicate that the type of adsorption and the driving force depends on the surface, a key feature when discussing asphaltene deposition. Adsorption of C5PeC11 onto silica is shown to be driven primarily by H-bonding ($\Delta H_z = -34.9 \, kJ/mol$) unlike adsorption onto calcite where polar Van der Waals and acidic/basic interactions are thought to be predominant ($\Delta H_z = -23.5 \, kJ/mol$). Interactions between C5PeC11 and stainless steel are found to be weak ($\Delta H_z = -7.7 \, kJ/mol$). Comparing C_6-asphaltenes and their esterified counterpart shows that adsorption at the liquid-solid surface is not influenced by the formation of H-bonds. This was evidenced by the similar adsorbed amounts obtained. Finally, C5PeC11 captures, to a certain extent, the adsorption interactions of asphaltenes present at the calcite- and stainless steel-oil surface.

1. Introduction

Among the many indigenous surface active compounds (resins, naphthenates, tetrameric acids) present in crude oil, asphaltenes receive special attention because they are largely responsible of several problems during production, transportation and refining of petroleum[1, 2]. For instance, asphaltenes are known to stabilize water-in-oil emulsions by forming a rigid and mechanically strong gel-like "skin" at the liquid-liquid interface that hinders coalescence and retards film drainage[3, 4, 5, 6, 7, 8]. Asphaltenes are also known to precipitate and, under certain conditions, create deposit layers that in some cases result in plug formation[9, 10, 11, 12]. This is perhaps one of the most undesirable problems encountered in oil production that leads to flow assurance issues and evidently, increases in operational costs. Asphaltene deposition is a complex phenomenon that is closely related to their adsorption onto solid surfaces such as, naturally occurring reservoir materials (e.g. clay and non-clay minerals, calcium carbonate) pipes, valves, wells, and other equipment[13, 14, 15, 16, 17]. Adsorption of a solute from a solution (e.g. asphaltenes from crude oil) is a physical phenomenon that is normally accompanied by a heat effect[18]. Hence experimental methods developed around

microcalorimetry that allow the determination of the adsorption enthalpy (ΔH_{ads}) are suitable for studying the adsorption mechanisms involved in these processes[19, 20].

Asphaltenes. They are typically defined as the solubility class of crude oil insoluble in *n*-alkanes (*n*-pentane, *n*-hexane) but soluble in aromatic compounds (xylene, toluene)[21, 22, 23]. Asphaltene adsorption at the liquid-solid surface has been studied for a wide range of surfaces[24, 25]. Differences in the adsorbed amounts, even at the same surface arise because asphaltenes are a polydisperse mixture in which the composition depends on crude oil origin[26]. Asphaltene adsorption generally induces an increase in the wettability of the solid surface.

From a study[26] on asphaltene adsorption from toluene solutions onto silicon wafers chemically modified with mixed self-assembled monolayers of various aliphatic and aromatic compounds, it was shown that increasing the number of carbon atoms (from 8 to 14) on the flat surface lead to a decrease in asphaltene adsorption. This strongly suggests that asphaltene adsorption is governed by interactions with the polar functionalities of the silicon wafers (SiOH groups). A similar study[27] concluded that the maximum adsorbed amount of asphaltenes (between 1.81 mg/m^2 and 3.78 mg/m^2) depends on polar interactions with the surface. These amounts can decrease sharply if the amount of Si-OH groups is altered[28]. By comparison with the adsorbed amounts onto $CaCO_3$ (calcite), the authors also concluded that an H-bond donor surface is not essential for adsorption to occur. Tayakout et al.[29] studied asphaltene adsorption onto two different alumina catalyst supports of different porosity and obtained a maximum adsorbed amount of 1.79 mg/m^2 at an initial bulk asphaltene concentration of 40 g/L. Acid-base interactions (Brønsted and Lewis acidity) and in particular, the acidity of these surfaces seems to be the key parameter for asphaltene adsorption at the solid-liquid surface[30, 31].

Adsorption of asphaltenes onto clay minerals such as kaolinite, illite and montmorillonite, and onto non-clay minerals such as quartz (SiO_2), calcite ($CaCO_3$), fluorite (CaF_2) and hematite (Fe_2O_3) has been of particular interest due to their retention capabilities in reservoir rocks[25, 32, 33, 34]. Generally speaking, adsorption onto non-clay minerals tends to be similar or higher than onto silica and alumina (1.0 mg/m^2-2.7 mg/m^2)[27, 35]; the adsorption mechanisms seem to be related to the hydration energies of the cations present (Mg^{2+}, Ca^{2+}, Na^+, K^+)[36] and interactions between asphaltenes and the polar groups (Si-OH, Al-OH)[25, 37]. Rankings of maximum adsorbed amount for these materials are commonly found in the literature and the

general trend is as follows[25, 37]: calcite (3.4 mg/m^2) > kaolinite (2.0 mg/m^2) > quartz (1.7 mg/m^2) > ilite (1.1 mg/m^2).

Adsorption of asphaltenes onto metal surfaces (stainless steel, iron and aluminum) which has high implications when discussing pipeline plugs and deposits, is normally characterized by higher adsorbed amounts compared to clay and non-clay minerals with values between [35] 2 mg/m^2 and 9 mg/m^2. The differences in adsorption capacities could be attributed to differences in the morphology of the particles which affect diffusion (porosity) and possibly electrostatic interactions.

Model compounds. The polydisperse and heterogeneous chemical nature of asphaltenes challenge a complete and thorough understanding of their properties. Sjöblom et al[38]. indicated two possible paths to assess this issue: (i) fractionation of the complete asphaltene content or (ii) synthesis of molecules that mimic the average chemical structure of asphaltenes. The first strategy probes challenging because asphaltene origin[11] and different precipitant/solvent mixtures (*n*-alkane/crude oil, *n*-heptane/toluene[39]) yield different –still– polydisperse fractions. The second strategy is a fundamental approach to design a molecule (or a family of molecules) that mimics the physical behavior of asphaltenes in terms of self-association, adsorption properties and establishes an ideal foundation for molecular simulations like MD. Asphaltene model compounds are based on the traditional "Archipelago" and "Continental" asphaltene models[40, 41, 42, 43]. The Archipelago model considers asphaltenes to have several aromatic sections attached to each other via alkyl chains. The Continental model states that polyaromatic hydrocarbons (PAHs) form a core to which aliphatic chains are attached[44, 45, 46, 47].

In a recently published review[38] on asphaltene model compounds, several studies were summarized. Three publications[44, 45, 46] focused on the study of asphaltene model compounds based on derivatives of pyrene which is a PAH consisting of four fused benzene rings. The main results showed that (I) the self-association properties studied varied significantly when compared to real systems (i.e. asphaltenes), (II) self-association could be enhanced if more alkyl side groups are added because bridged structures have the tendency to counteract it and (III) Self-association properties in model compounds cause them to be present as dimers (whereas in the case of indigenous asphaltenes it happens via higher aggregation states). This is due to H-bonds and π-π stacking interactions involving the pyrene rings and a bypiridine spacer.

Two important studies[47, 48] concluded through molecular dynamic modeling (MD) that molecules with charged terminal groups are tethered to the toluene-water interface contrary to the uncharged compounds, and that the stacked polyaromatic rings are orthogonally oriented to the same surface. These results are in agreement with experimental results on a different family of model compounds of the perylene-basedtype[49, 50, 51]. This family of model compounds showed that central properties of indigenous asphaltenes can be reproduced. First, the solubility in heptane-toluene mixtures of the model compound C5Pe (*N*-(1-hexylheptyl)-*N'*-(5-carbonylicpentyl) perylene-3,4,9,10-tetracarboxilic bismide) which has an acidic end group, is comparable to that of asphaltenes. Second, C5Pe adsorption at the liquid-liquid interface suggests that only a fraction of asphaltenes are responsible for the observed surface activity and the importance of carboxylic functionalities. Third, studies at the water-air interface through a Langmuir trough and images obtained via Brewster Angle Microscopy (BAM) indicated that the carboxylic groups adopt a *head-on* conformation with a face-to-face packing of the core. That is, the acidic group immersed into the aqueous phase and the polyaromatic cores "stacked" orthogonally to the surface. And fourth, as recently shown by Bi et al.[52] C5Pe is prone to the formation of heterogeneous interfacial films at the xylene-water interface which leads to stable W/O emulsions. Furthermore, BAM and atomic force microscopy (AFM) images showed that rearrangements and accumulation at the interface lead to the progressive build-up of the layer, generating a mechanically strong film. It is evident that a great amount of the adsorption properties of asphaltenes can be successfully mimicked by perylene-based model compounds such as C5Pe.

In this work, adsorption of asphaltenes and asphaltene model compounds (similar to the previously described C5Pe) at the solid-liquid surface is systematically studied and compared to determine the forces and type of interactions between these species and solid surfaces involved in the adsorption process. Adsorption isotherms coupled with the enthalpies of adsorption at three different representative surfaces, namely silica, calcite and stainless steel, provide a broad approach to the adsorption mechanisms involved in real and model systems. The relationship between interactions at the solid-liquid surface and the energy involved in asphaltene adsorption is of paramount importance to address the driving force for adsorption and the predominant type of bonding. Besides the work of Tabrizy et al.[19] there seems to be very few studies on this subject.

2. Materials and methods

Solvents and chemicals.

All chemicals involved in the synthesis of the model compounds are described thoroughly by Wei et al.[53] Toluene (99.8%, anhydrous) used to prepare all asphaltene, esterified-asphaltenes and asphaltene model compound solutions; Chloroform (ACS reagent, purity ≥ 99.8%) and Acetic Acid (ReagentPlus®, purity ≥ 99%) used for High-performance Liquid Chromatography (HPLC) measurements were purchased from Sigma-Aldrich. Hellmanex III (Helma Analytics), ethanol (VWR, 96%) and Sodium dodecyl sulfate salt (Merck, ≥ 99%) were used for cleaning the QCM crystals. All chemicals were used as received.

Asphaltene model compounds.

Two asphaltene model compounds were used for this work. The first one, named C5PeC11, has an acidic functionality and is very similar to the previously mentioned C5Pe; the difference is the longer aliphatic chains that enhance its solubility in toluene. The second one, named BisAC11 has low to none interfacial activity and an aliphatic end-group. C5PeC11 was synthesized following the 4-step procedure described in Nordgård et al.[51] and Holman et al.[54] and by changing 7-tridecanone to 12-tricosanone; 12-tricosanone is first treated with ammonium acetate and sodium cyanoborohydride in isopropyl alcohol to convert it into its corresponding amine. The amine is then reacted with perylene-3,4,9,10-tetracarboxylicdianhydride in the presence of imidazole. This step yields BisAC11 as an intermediate product. BisAC11 is further treated with potassium hydroxide in tert-butanol to obtain a mono-substituted intermediate after purification by flash chromatography. This compound is then reacted with 6-aminohexanoic acid in the presence of imidazole. The final product, C5PeC11, is hence obtained and purified by flash chromatography on silica gel using a methanol-chloroform mixture (0-5% in $CHCl_3$) as eluent. Table 3 provides the chemical structure and the molar mass of the model compounds of this study.

Intermediate and final products were characterized by ^1H NMR spectroscopy in $CDCl_3$. All the peaks are accounted for and yield a match with the expected chemical structure; hence the purity of these compounds is assumed to be very high. The ^1H NMR spectra of BisAC11 and C5PeC11 are presented in Fig. S1 and Fig. S2 of the supplementary material respectively.

Asphaltenes.

C_6-asphaltenes were extracted with *n*-hexane from a solvent/chemical-free heavy crude oil of the Norwegian continental shelf. The process is as follows: first, the crude oil is heated to

60°C for 24 h. Then, the crude oil is diluted in *n*-hexane at a 1:40 weight/volume ratio. The mixture is stirred for 24 h and the asphaltene fraction is recovered using a 0.45µm HVLP (Millipore) membrane filter washing with excess *n*-hexane. Finally, the recovered asphaltenes are put into a nitrogen atmosphere degasser and dried for 48 h. This time is enough to ensure that the solvent is fully evaporated which means that the mass of the samples is constant. Basic analysis of the crude oil used in this study and the elemental composition of the extracted asphaltenes is given in Tables 1 and 2.

Asphaltene esterification.

Esterification of asphaltenes was performed using the procedure described by Nasir et al.[55] 0.5 g of C_6-asphaltenes were dissolved in 10 mL of CH_2Cl_2 and stirred for 30 minutes in a sealed flask. After this step, 50 mL of H_2SO_4 (2 %w/w) in methanol were added to the first solution and refluxed at ~63 °C for 3 h under nitrogen. The mixture was allowed to cool down to room temperature, point at which 100 mL of mili-Q water were added. The asphaltene-rich phase was then extracted by flushing 100 mL of CH_2Cl_2 3 times in a separation funnel. Finally, this phase was washed with 40 mL of $NaHCO_3$ (2 %w/w). The solid esterified asphaltenes were obtained after evaporation of CH_2Cl_2 and a drying step under nitrogen. The mass yield was ~99.5%.

The esterification was characterized by FTIR spectroscopy using in a Bruker Optics spectrometer (Germany) equipped with an attenuated total reflection (ATR) cell. The spectra were collected from asphaltene and esterified asphaltene concentrated solutions in CH_2Cl_2 between 4000 and 600 cm^{-1}after 64 scans at a resolution of 2 cm^{-1}. Further details of this characterization can be found in the supplementary material (Fig. S3) and on Simon et al[56].

An additional study was performed by esterification of 4-heptylbenzoic acid (Sigma-Adrich) using the same procedure as for asphaltenes to verify the efficiency of the esterification procedure. This step served as validation of the procedure because the concentration of – COOH groups in asphaltenes is significantly lower than in a pure acid. The same FTIR peaks were observed. ^{1}H NMR spectroscopy in $CDCl_3$ was also performed and all the peaks are accounted for corresponding to an ester structure and corroborating that the replacement (methylation) of the Hydrogen atom in the –COOH groups was complete.

Solid surfaces.

Three solid surfaces, representative for different stages in oil production were used in this study. Fumed and chemically flocculated silica particles (Aerosil 200) was kindly provided by Evonik Industries (Germany). Calcium carbonate ($CaCO_3$, calcite confirmed by XRD spectrum) particles were purchased from Specialty Materials, USA. Stainless steel nanoparticles (316L) were purchased from SkySpring Nanomaterials Inc. Table 4 shows the main features of the particles.

The specific surface area of the particles was determined via gas adsorption. The method was carried out in a Micromeritics TriStar 3000 instrument equipped with a N_2 adsorption/desorption system operated at 77K. Prior to the measurements, the samples were degassed under vacuum at 300°C for 24h (except for stainless steel particles which were degassed under vacuum at room temperature). After measuring the adsorption/desorption isotherms, the data were automatically fitted using the BET equation. Table 4 shows the obtained values. Additionally, thermogravimetric analysis did not show any presence of water in the temperature range studied.

Calcium carbonate and silica particles were treated before use to ensure that water was not present when preparing the solutions. The pre-treatment was as follows: first the particles were placed in an oven at 120°C for 24h. And second, the particles were cooled down in a desiccator in the presence of silica gel for ~4h. It is important to mention that this pre-treatment was carefully performed for every measurement and that stainless steel particles were not pre-treated due to the changes in physical appearance and specific surface area observed after thermal treatment.

The equilibrium contact angle of three different coated quartz crystals was measured with a CAM 200 (KSV Instruments, Finland) device. The measurements were performed at the solid/liquid/air interface at room temperature (22°C) by placing a drop of Milli-Q water onto the crystal with a syringe. 40 images taken after 40ms were automatically analyzed and yielded the average values reported in Table 4. The quartz crystals used were: SiO_2 (QSX 303, Q-Sense), calcium carbonate (QSX 999, Q-Sense) and stainless steel SS2343 (QSX 304, Q-Sense), equivalent to silica, calcium carbonate and stainless steel particles respectively.

Adsorption isotherms.

Adsorption isotherms of asphaltenes and asphaltene model compounds were determined by the solution depletion method (DM). The surface-to-volume ratio (S/V) for each particle was

kept constant at 5.1×10^5 for silica, 2.6×10^5 for calcite and 1.1×10^5 for stainless steel (amounts are in m^{-1}). The procedure was as follows: first, the pre-treated particles were weighted in 40mL PFTE screw-cap glass vials. Second, the required amount of solution (asphaltene or asphaltene model compound) in toluene was added. The initial bulk concentration ranges were: [0.2-1.5] g/L for asphaltenes, [0.4-1.5] g/L for C5PeC11 and [0.1-1] g/L for BisAC11. Third, the vials were immersed in a water bath at $25 \pm 0.1°C$ for 24h. During this stage, the mixtures were constantly stirred with the help of a magnetic stirrer. Fourth, the supernatant of the mixtures was filtered using a PFTE-syringe filter (Acrodisc 0.2μm -25mm HPLC certified, Sigma-Adrich). HPLC measurements confirmed that the model compounds are not retained in the filters during this step. Finally, the concentration of the filtered solution (and also before adsorption) was determined via HPLC* for C5PeC11 and UV spectrophotometry** for BisAC11 and asphaltenes. The adsorbed amount was calculated using equation (1)[49].

$$\Gamma_{ads} = \frac{(C_i - C_{eq})V}{m_p A_p} \tag{1}$$

In this equation, $\Gamma_{ads}(mg/m^2)$ is the surface concentration, C_i and $C_{eq}(g/L)$ are the initial and equilibrium concentration of the solute in the oil phase volume (i.e. asphaltenes or model compounds) before and after adsorption respectively, $V(L)$ is the volume of the oil phase, $m_p(mg)$ is the mass of particles used and $A_p(m^2/g)$ is the specific surface area of the particles.

Determination of the concentration via HPLC.

The modules used to build the HPLC system used in this study are thoroughly described in Simon et al[57]. For this work, a Phenomenex column (Luna 5μ silica 100Å 250 x 4.6mm) was used at a controlled temperature of $25 \pm 0.1°C$. Data were collected and analyzed using a Shimadzu LC solution v.1.22 SP1 software. Elution was performed using an isocratic flow of $CHCl_3$ and Acetic acid at 0.96 and 0.4 mL/min respectively as the mobile phase. UV detectors at 260 and 323nm yielded a C5PeC11 peak at ~6.5min.

Determination of the concentration via UV spectrophotometry.

A UV-Spectrophotometer (Shimadzu UV-2401PV) in absorbance mode was used to determine the concentration before and after adsorption of BisAC11 and asphaltene solutions in toluene. A 10mm quartz cuvette was used for all measurements. For BisAC11 the

absorbance values at 458 and 490nm were used to calculate the concentration. In the case of asphaltenes, the absorbance values at 500 and 600nm were used.

Quartz crystal microbalance with dissipation (QCM-D) experiments.

Adsorption of asphaltenes and esterified asphaltenes onto coated-quartz crystals of stainless steel and silica was measured using quartz crystal microbalance with dissipation (QCM-D). The apparatus used was single sensor microbalance system Q-sense E1 from Biolin Scientific (Sweden).

The stainless steel coated-crystals were cleaned prior to use as follows: first, the crystal was immersed in solution of 1% hellmanex in water for at least 1 h. Second, the crystals were washed with milli-Q water followed by a sonication step in ethanol for 10 min. Finally, the crystals were dried with N_2 and treated in a UV-chamber for 15 min. The silica coated crystals were cleaned using a similar procedure except that the initial solution was 2% sodium dodecyl sulfate in water and no sonication in ethanol was performed.

QCM-D adsorption experiments were performed with the following procedure: Toluene is initially passed through the chamber containing the crystal at 20°C to obtain a baseline. The baseline was considered to be stable if the frequency change was less than ±1 Hz for 10 min. Solutions of non-esterified asphaltenes or esterified asphaltenes in toluene were then injected into the chamber in a stepwise manner using a pump (flow rate = 750 µL/min). The initial bulk concentration range of these solutions was [0.2-1.5] g/L. Sample injection time was 10 min followed by a waiting time of 5 min before the next sample injection was performed. The QCM-D experiments were performed by duplicate.

The QCM-D operates based on the property of piezoelectricity. The piezoelectric quartz crystal coated with stainless steel (or silica) is located between two metal electrodes. By applying an AC voltage across the electrodes, the crystal is excited to oscillate. The frequency of oscillation depends on the mass adsorbed onto the surface of the crystal. The relationship between the change in frequency (Δf) due to the mass adsorbed (Δm_{ads}) was established by Sauerbrey[58] through equation (2):

$$\Delta m_{ads} = -\frac{\rho_q t_q}{f_o n}\Delta f = -\frac{\rho_q v_q}{2f_o^2 n}\Delta f = -\frac{C}{n}\Delta f = \Gamma_{ads} \tag{2}$$

Where $\rho_q = 2648 \text{ kg/m}^3$ and $t_q = 0.3 \, mm$ are the mass density and thickness of the crystal respectively, $v_q = 3340 \, m/s$ is shear wave velocity in quartz, $f_o = 5 \, MHz$ is the fundamental frequency of crystal and n is the overtone number. The constant C equals to 0.177 mg·m^{-2}·Hz^{-1}. In the present study, the overtones 3, 5 and 7 are considered. The Sauerbrey equation is valid only when the mass adsorbed is evenly distributed on the surface, Δm_{ads} is smaller than the mass of the crystal and the adsorbed mass is rigidly attached to the surface[58].

The change in dissipation due to adsorption is given by equation (3)[59]:

$$D = \frac{E_{dissipated}}{2\pi E_{stored}} \tag{3}$$

Where D is the dissipation factor, $E_{dissipated}$ is the energy dissipated during one period of oscillation and E_{stored} is the energy stored in the oscillating system. In the case of formation of viscoelastic films on the surface, the Sauerbrey relationship equation (2) is no longer valid.

Adsorption enthalpies.

The adsorption enthalpies (ΔH_{ads}) were determined by a titration method in a cell placed into a Tian-Calvet type microcalorimeter, TAM III provided by TA instruments. In an experiment, between 3 mg and 70 mg of the powder (i.e. silica, calcite or stainless steel) are placed in a stainless steel cell and treated in an oven at 120°C for 24h in order to provide the same thermal treatment as for the adsorption isotherms. The stainless steel particles are not treated. After cooling, dry toluene is introduced in the cell. The cell is then fixed on the calorimetric titration set-up and introduced into the thermopiles. After thermal equilibrium and while keeping the system stirred, a stock solution of the studied species (i.e. asphaltenes or asphaltene model compounds) is introduced step by step into the calorimetric cell. The initial bulk concentrations of the solutions were: 2.4 g/L (C5PeC11), 5.8 g/L (BisAC11) and 2.6 g/L (C$_6$-asphaltenes). This process yields a calorimetric peak that contains two contributions: one of adsorption and one corresponding to a dilution effect. The heat of dilution contribution is calculated from a blank experiment without the particles. A homemade software is used to calculate the dilution contribution, the amount adsorbed in the calorimetric experiment and the enthalpy of adsorption. This is done by starting from the experimental data: heat measured at each injection, the adsorption isotherm and the dilution enthalpy curve. Around 20 injections of 10µL of stock solution are performed with 1h

equilibrium time. Pseudo-differential enthalpies of adsorption are determined through the use of small adsorption steps.

3. Results and discussion

Adsorption isotherms onto silica, $CaCO_3$ (calcite) and stainless steel particles for the acidic asphaltene model compound C5PeC11 and C_6-asphaltenes are first presented. Adsorption onto silica of the model compound BisAC11, which has an aliphatic end-group and no acidic functionality follows. The corresponding heat of adsorption for C5PeC11 and C_6-asphaltenes measured by microcalorimetry experiments is presented after. Finally, the adsorption of esterified- and non-esterified asphaltenes obtained through QCM-D experiments is presented to elucidate the effect of acidic functionalities on adsorption at the liquid-solid surface. With this framework, the driving force for adsorption and the predominant type of bonding involved at each surface are thoroughly studied and discussed. Comparison between the asphaltene model compounds and indigenous asphaltenes will give an overview of the adsorption properties that can be mimicked by these model compounds.

3.1 Adsorption isotherms.

Adsorption isotherms of C5PeC11 and C_6-asphaltenes onto three different surfaces are shown in Fig. 1 and Fig. 2. The equilibrium concentration (C_{eq}) was measured via HPLC for C5PeC11 and via UV-spectrophotometry for asphaltenes. It is clear from these figures that the shapes are not completely similar. Both systems exhibit an increase in the surface concentration with equilibrium concentration followed by a plateau zone typical of a Langmuir type-I shape. In the specific case of C5PeC11, it reaches ~90% of the plateau value in a narrower concentration range (0-0.05 g/L vs 0-1 g/L). This means that the model compound C5PeC11 exhibits a much higher surface affinity than asphaltenes. The plateau values (Γ_p) for C5PeC11, also shown in Table 4, are higher for all surfaces except for silica, where C5PeC11 saturates the surface faster but reaches a slightly lower saturation value (1.32 mg/m^2 vs 0.91 mg/m^2). In all cases, adsorption capacities at the liquid-solid surface can be ranked as follows: stainless steel > calcium carbonate > silica. This ranking is consistent with what has been reported for asphaltenes[25, 27, 35] which suggests that the model compound C5PeC11 falls into this feature.

Another interesting aspect of Fig. 1 and Fig. 2 is that the adsorbed amount of asphaltenes onto the surfaces seems to be more similar to each other than for C5PeC11 given that the

plateau values are within a short range (1.36 mg/m^2-1.99 mg/m^2) while C5PeC11 exhibits a larger range (0.95 mg/m^2 - 4.0 mg/m^2). These differences suggest that the different polydisperse sub-fractions of asphaltenes (for instance acidic and basic) interact in a way so as to yield an average behavior. This highlights the importance of determining the major agents that influence adsorption onto various surfaces. On the other hand, C5PeC11 is a single well-defined molecule with low polydispersity that shows the influence of an acidic end-group in adsorption.

Adsorption of BisAC11 onto silica particles is presented in Fig. 3. It is clear from the figure that this model compound exhibits a very low adsorption capability due to its aliphatic end groups (Table 3). In fact, the adsorbed amount of BisAC11 is roughly 100 times lower than C5PeC11 suggesting that this model compound does not adsorb at the solid-liquid surface. An interesting observation in Fig. 3 is that two different surface-to-volume ratios (S/V) were tested. This was done to increase the total surface area of the particles and to emphasize that the low adsorbed amounts are not due to the low concentration difference between before and after adsorption. These types of model compounds could be representative of those asphaltene sub-fractions that are not surface active but induce polydispersity.

3.2 Heat of adsorption.

The adsorption enthalpies of C5PeC11 are plotted in Fig. 4. They are in the reverse order of adsorption capacity showing the highest values for silica. This is in agreement with the polar character of the surfaces as defined by the contact angle measured on quartz crystals and also shown in Table 4. C5PeC11 has an acidic functionality that can interact with SiOH groups. In a preceding paper[60], it was shown that the adsorption enthalpy of an acid function onto silica, from ethanol as solvent, was above -20 kJmol^{-1}. The values obtained here are (ca. -35kJmol^{-1}) hence not so surprising. The enthalpy value slightly decreases when the coverage increases, which is the usual behavior for heterogeneous surfaces. Nevertheless it could also indicate that the conformations (orientations) of the adsorbed molecule change when coverage increases as in the case of polymers[61]. In the case of Asphaltenes shown in Fig. 5, the behavior is different both in amplitude (adsorption enthalpies are rather lower than in the case of C5PeC11) and in evolution. The enthalpy here increases with coverage showing a non-negligible contribution of lateral interactions between molecules. An average value of 750 g/mol for asphaltene molecular weight was used for the calculations. It is important to highlight that the use of this value for the discussion of the adsorption enthalpy in the next

section implies that it is assumed that single individual monomers of asphaltenes are being adsorbed and not asphaltene aggregates.

3.3. Discussion.

Based on the results presented in the previous sections, the discussion can therefore be centered on the nature of interactions (based on the heat of adsorption) present during adsorption of model compounds and asphaltenes at the solid-liquid surface. The data on Fig. 4 and Fig. 5 can be semi-quantitatively described by equation (4):

$$\Delta H_{ads} = mC_s + \Delta H_z \qquad (4)$$

Where ΔH_{ads} is the differential adsorption enthalpy measured and C_s is the adsorbed surface concentration. The fitting parameter m is a characteristic quantity that represents either lateral interactions (when the general trend of the adsorption enthalpy is to increase with concentration) or rearrangements at the surface combined with possible lateral interactions enhanced by surface heterogeneity when the tendency of the adsorption enthalpy is to decrease with the concentration. The fitting parameter ΔH_z is the value of the adsorption enthalpy at infinite dilution or at zero coverage. This parameter can be seen as a value representative of the molecule, aggregate or cluster in its highest interaction with the surface. These two fitting parameters are also shown in Table 4 for each surface. As stated on section 3.2, the value of the average molecular weight used for asphaltenes implies that the calculated ΔH_z corresponds to the adsorption of single individual monomers. It is known that asphaltenes have the tendency to self-associate in the bulk even at concentrations as low as 100 mg/L[62] and so if this process takes place, that is, if the measured enthalpy of adsorption corresponds to the adsorption of asphaltene aggregates, it follows that the enthalpy values would decrease. This important aspect should be kept in mind for the following discussion.

An important aspect of Fig. 4 and Fig. 5 is that ΔH_{ads} for C5PeC11 has the slight tendency to decrease with the concentration for all surfaces. This is indicative of the almost negligible presence of lateral interactions at the surfaces. On the other hand, ΔH_{ads} for C_6-asphaltenes has the tendency to increase with the surface concentration. This trend is a clear indication of self-association, multi-layer formation, strong lateral interactions and eventually the presence of rearrangements at the surfaces[20]. Similar phenomena have been observed previously through different techniques at the liquid-liquid[63, 64] and liquid-air[50] interface for asphaltenes supporting these observations. Similarly, Table 4 shows that for C5PeC11 and C_6-asphaltenes

there is a correlation between the contact angles of the quartz crystals (a measure of their hydrophobicity), the adsorbed amount in the plateau region Γ_p and the enthalpy at zero coverage ΔH_z.

Asphaltene and C5PeC11 adsorption onto silica, calcite and stainless steel can be summarized as follows. (I) The adsorbed amount and the contact angle are ranked as: stainless steel > calcite > silica for both species. (II) The relationship of these two variables with the heat of adsorption in C5PeC11 follows the opposite trend (silica > calcite > stainless steel) and it tends to decrease as the surface concentration increases. In the following sections, each surface is analyzed individually to expand on these remarks.

Adsorption onto silica.

The first case to consider is adsorption of C5PeC11 and C_6-asphaltenes onto silica. It is not surprising that C5PeC11 has the highest value for the fitting parameter $\Delta H_z = -34.9 \; kJ/mol$ (Table 4) onto this surface. There is a large driving force for adsorption that arises from the difference between a highly apolar bulk (solutions in toluene) to a highly polar surface (contact angle = 5.5° measured at flat surfaces and not at the particles). The nature of the interaction between C5PeC11 and silica seems to be related mostly to H-bonding which provides interactions energies of ca. -20 kJ/mol[65] coupled with multiple π—π (ca. -16 kJ/mol)[66] and dipole—dipole interactions (ca. -2 kJ/mol)[66]. Additionally, the energy of dimerization of C5PeC11 in xylene has been determined[67] to be ca. -45 kJ/mol. In this case, the main contribution to the adsorption energy comes from strong interactions between the –COOH groups from the model compound and the SiOH groups of the surface.

Contrary to C5PeC11, the enthalpy at zero coverage for C_6-asphaltenes is rather low: $\Delta H_z = -8.9 \; kJ/mol$. This clearly indicates that the nature of the interactions between the different functionalities present in asphaltenes and the SiOH groups of the surface are different. Furthermore, from this value it can also be stated that the nature of the interactions is not related to H-bonds. The parameter m also indicates that these interactions are not significant as the concentration increases. This remarkable aspect of adsorption at the liquid-solid surface which also happens to be fundamentally different to adsorption at the liquid-liquid interface is further assessed in a later section in which the influence of –COOH groups in adsorption is evaluated. These acidic functionalities (ionized form) seem to be largely responsible for the interfacial behavior especially at low contact angle surfaces (highly hydrophilic)[68].

Adsorption onto stainless steel.

Adsorption of C5PeC11 and C_6-asphaltenes onto stainless steel is the lowest in energy (Fig. 4 and Fig. 5) but the highest in adsorbed amount (Fig. 1 and Fig. 2). This particular result arises from the lower driving force involved. The contact angle of the stainless steel flat surface is ca. 56° (Table 4) which means that the surface is more hydrophobic than silica, thus the interactions between the species and surface are less energetic: $\Delta H_z = -7.7\ kJ/mol$, $m = -4.0\ kJm^2/mol^2$ for C5PeC11 and $\Delta H_z = -4.6\ kJ/mol$, $m = 11.9\ kJm^2/mol^2$ for C_6-asphaltenes. In both cases, it is clear that H-bonding and π—π stacking are not involved in adsorption resulting in the absence of strong attractive interactions especially if acidic groups are not present. This means that for C5PeC11 and C_6-asphaltenes the interactions between -COOH groups with the stainless steel surface are not responsible for adsorption. Comparison to oil-water interfaces in which values of ~10 mg/m^2 [69] and ~2.7 mg/m^2 obtained with Athabasca and Cold Lake asphaltenes[70] have been reported, the value ~1.94 mg/m^2 obtained in this study could be evidence of this phenomenon. Electrostatic interactions provided by elements such as chromium, nickel, silicon, carbon and heteroatoms such as sulfur and phosphorus present in the structure of stainless steel coupled with the surface charge of asphaltenes[71] has also been suggested[70] as possible mechanism that enhances adsorption. This would be in agreement with the obtained energy values of Fig. 4 and it would explain why C5PeC11 exhibits a higher adsorbed amount. A third aspect that could influence the adsorbed amount is penetration. If the particles exhibited a certain degree of porosity, large asphaltene aggregates would not be able to access the entire nano-powder surface area of heterogeneous morphology whereas the single un-aggregated C5PeC11 molecules could penetrate further enhancing adsorption

Adsorption onto CaCO$_3$ (Calcite).

The final case of this section is that of Calcite which exhibits an intermediate behavior in all aspects. The heat of adsorption is similar for C5PeC11 and C_6-asphaltenes suggesting the presence of similar mechanisms of adsorption at the calcite-liquid surface. The driving force between the bulk solutions and the intermediate hydrophobicity (contact angle of the flat surface ca. 21°) causes intermediate values for ΔH_z (Table 4). Adsorption onto calcite could be attributed largely to polar interactions between the carboxylic groups present in asphaltenes (and C5PeC11) and the positively charged (or neutral)[72] calcite surface that is sometimes regarded as weakly basic[19, 73]. The order of magnitude of the measured adsorption

energies is also consistent with the presence of π—π stacking which is expected on acidic molecules/species with polyaromatic rings. ΔH_z for both species could also indicate the presence of H-bonds however it will be shown that this is not the case when adsorption of esterified asphaltenes is assessed.

Going back to the remarks stated at the beginning of this section, it is also possible to state that: (III) In the case of C_6-asphaltenes, the tendency of the heat of adsorption is to increase with surface concentration indicating the presence of rearrangements and lateral interactions after adsorption (also evidenced with the increasing *m*-values). The trend in the heat of adsorption according to the surface (calcite > silica > stainless steel) is different in the case of silica suggesting a different influence of the acidic groups on interfacial properties. (IV) The heat of adsorption of C5PeC11 and C_6-asphaltenes onto calcite and stainless steel particles is similar suggesting that the model compound captures important properties of indigenous asphaltenes and therefore it can be used as a representative model system. Adsorption onto calcite and stainless steel are different in nature and mainly attributed to polar interactions and electrostatic bonding respectively. Adsorption onto silica is not fully mimicked mainly due to the more pronounced effect of a single acidic molecule (C5PeC11) compared to the polydisperse response of asphaltenes.

Influence of –COOH groups in adsorption.

It is clear from Fig. 1 and Fig. 4 that adsorption at the liquid-solid surface of the asphaltene model compound C5PeC11, which has an acidic functionality, seems to be driven by H-bond polar interactions (silica and possibly calcite) and by electrostatic bonding (stainless steel). In the case of C_6-asphaltenes, adsorption seems to follow a similar trend; however the picture is not completely clear. Asphaltene adsorption at the liquid-liquid interface has been shown to be pH-dependent (crude oil as well)[68]. At high pH values, asphaltenes become highly surface active causing a dramatic reduction of the interfacial tension, whereas at neutral pH the response is very low. In fact, it has been shown that at neutral pH, the interfacial tension reaches the highest value[74]. Furthermore, the stability of asphaltene-emulsions seems to correlate with this trend[75]. This behavior has been largely attributed to the influence of –COOH groups and their subsequent ionization in aqueous phase.

To correctly assess the influence of -COOH groups on asphaltene adsorption at the liquid-solid surface (no aqueous phase present), C_6-asphaltenes were esterified and their solutions in toluene studied (see Fig. S3 of the supplementary material). Fig. 6 shows the obtained

esterified asphaltenes (E-Asph) isotherms by the depletion method (DM) with stainless steel and silica particles. The non-esterified asphaltenes (Asph) isotherms are also shown for comparison. It is clear from this figure that these isotherms are very similar suggesting that the influence of –COOH groups in asphaltene adsorption at the liquid-solid is negligible. However, it could be argued that the amount of acidic groups in the asphaltene fraction might be too low to be manifested throughout this method. In such case, the absence of selectivity for adsorption of esterified asphaltenes seen in Fig. 6 could be attributed to the adsorption of a large proportion of the initial asphaltene content present in solution (with $\Delta c/c$ between 8-80%) which would represent more than the total acidic asphaltene sub-fraction. A simple calculation using the total acid number (TAN) of the asphaltenes in this work (7.60 mg/g as reported by Simon et al.[56]) and an average molecular weight of 750 g/mol shows that there is approximately 1 acidic asphaltene molecule per 10 non-acidic asphaltene molecules, which is indeed rather low.

To evaluate the previous argument, QCM-D experiments were performed and the resulting isotherms are presented in Fig. 6 under the labels "QCM". The low surface-to-volume ratio (S/V) of the measuring cell ensures that depletion of asphaltene material during the adsorption experiments remains negligible[35, 76]. Consequently, the possible influence of a particular sub-fraction of asphaltenes (i.e. acidic, basic) should be more visible than in typical depletion experiments. An important aspect of Fig. 6 regarding QCM-D results is that the adsorption ranking remains the same compared to the depletion experiments (even though the total adsorbed amount is higher in all cases), that is, stainless steel > silica for both esterified and non-esterified asphaltenes. The reasons behind this difference in the total adsorbed amount for the same surfaces between QCM-D measurements and DM is not fully understood yet. However, different explanations could be put forward to attempt an explanation. For instance, the interactions between asphaltenes and the solvent might induce a transition from the colloidal regime (present at low concentrations) to a much larger swollen regime[77] that would give rise to an apparent higher mass in QCM-D measurements. Second, as it will be mentioned shortly, asphaltenes are partly irreversibly adsorbed at the solid-liquid surface. Hence changes in the S/V ratio could cause a high impact on the measured adsorbed amount because equilibrium might not be reached. And third, it is possible that in the case of silica, the difference between adsorption onto particles and QCM-D crystals is due to the changes in the density of silanol groups. In the case of stainless steel,

this difference could be due to the aggregated state of the particles, thus reducing the available area for adsorption in DM measurements.

The main feature of Fig. 6 is however that adsorption of esterified and non-esterified asphaltenes onto the stainless steel and silica crystals is essentially the same. This indicates, once more, that unlike asphaltene adsorption at the liquid-liquid interface, the influence of − COOH (non-ionized) groups at the liquid-solid surface is not preponderant. The adsorption enthalpy results presented in Fig. 5 are in agreement with this statement given that the energies are significantly lower than those of polar interactions.

The above analysis and results are consistent with the experimental results obtained with silica and stainless steel particles. It is clear from the energy evaluation that C5PeC11 adsorption onto silica, unlike asphaltenes, is dominated by H-bonds since BisAC11 has a negligible adsorption at the oil-silica surface. This consequently causes a big reduction in ΔH_z. In the case of stainless steel, the influence of H-bonds is negligible which is coherent with the similar values of ΔH_z obtained for asphaltenes.

Finally, the reversibility of asphaltene adsorption was also studied through QCM-D experiments (not through the depletion method experiments). Table S1 of the supplementary material shows the weight percentage of mass desorbed after 3 washout cycles with pure solvent (toluene) performed after injection of the most concentrated solution (1.5 g/L). It is clear from this table that asphaltenes are partly irreversibly adsorbed at the stainless steel- and silica-oil surface given that the values do not exceed~22% and further washouts have no effect. This behavior could be due to the relevant interactions between asphaltenes in the adsorbed layer.

4. Conclusions

Adsorption isotherms and contact angle measurements showed that C_6-asphaltenes and the model compound C5PeC11, which has an acidic functionality, can be ranked as follows: stainless steel > calcite > silica. The similarities in the adsorption ranking indicate that the model compound captures the adsorption affinity order of indigenous asphaltenes at the liquid-solid surface.

The driving force that arises from the apolar bulk solutions and the different hydrophobicity of the surfaces provides an indication of the nature of the interactions that dominate adsorption. The heat of adsorption, characterized by the parameter ΔH_z of equation (4), for

C5PeC11 onto silica (-34.9 kJ/mol) and calcite (-23.5 kJ/mol) are compatible with the formation of H-bonds (possibly not for calcite), polar interactions and π—π stacking. These values at zero surface coverage can be taken as the initial energy of adsorption even though the state of the adsorbing molecules (for example aggregation) is unknown. On the contrary, the heat of adsorption of C5PeC11 onto stainless steel is significantly weaker (7.7 kJ/mol) to be considered as a type of polar interaction. It is speculated based on the values that adsorption onto this surface could be due to electrostatic interactions.

The adsorption enthalpy for C_6-asphaltenes increases with surface concentration which is typical of lateral interactions and aggregation. This could also indicate the formation of a multi-layered structure, characteristic of asphaltenes. On the other hand, the adsorption enthalpy for C5PeC11 slightly decreases with the surface concentration which is indicative of rearrangements at the liquid-solid surface or differences in the surface sites. Self-association is one of the aspects in which the work on model systems that mimic real asphaltene behavior needs to be extended to provide similar aggregation states and polydispersity.

Unlike asphaltene adsorption at the liquid-liquid interface (which is pH dependent), the presence of –COOH groups in the asphaltene fraction does not seem to have a strong influence on adsorption at the liquid-solid surface. Varying the S/V ratio to avoid depletion effects did not produce any significant difference in the isotherms, suggesting that the acidic sub-fraction of asphaltenes has little influence. Keeping in mind the intrinsic limitations associated with using a model system, in this case, molecules with defined chemistry to approach a polydisperse-interacting system such asphaltenes, the results show that the asphaltene model compound C5PeC11 has potential as an adequate approximation for asphaltene adsorption at the calcite- and stainless steel-oil interface and not so representative for adsorption onto silica. An important difference between C5PeC11 and C_6-asphaltenes was made evident through Fig. 6: adsorption of the model compound is driven by –COOH interactions while these interactions have negligible influence on adsorption of indigenous asphaltenes at the solid-liquid surface.

Acknowledgements

References

1.   Speight, J. G. Exploration, Recovery, and Transportation. In *The Chemistry and Technology of Petroleum*, Fourth Edition ed.; CRC Press. Taylor and Francis group, LLC: Boca Raton, 2007.
2.   Kilpatrick, P. K. Water-in-Crude Oil Emulsion Stabilization: Review and Unanswered Questions. *Energy & Fuels* **2012,** *26* (7), 4017-4026.
3.   Simon, S.; Jestin, J.; Palermo, T.; Barre, L. Relation between solution and interfacial properties of asphaltene aggregates. *Energy and Fuels* **2009,** *23* (1), 306-313.
4.   Jeribi, M.; Almir-Assad, B.; Langevin, D.; Hénaut, I.; Argillier, J. F. Adsorption kinetics of asphaltenes at liquid interfaces. *Journal of Colloid and Interface Science* **2002,** *256* (2), 268-272.
5.   Pensini, E., Harbottle, D., Yang, F., Tchoukov, P., Li, Z., Kailey, I., Behles, J., Masliyah, J., Xu, Z. Demulsification Mechanism of Asphaltene-Stabilized Water-in-Oil Emulsions by a Polymeric Ethylene Oxide–Propylene Oxide Demulsifier. *Energy & Fuels* **2014**.
6.   Zhang, L. Y.; Xu, Z.; Masliyah, J. H. Langmuir and Langmuir-Blodgett films of mixed asphaltene and a demulsifier. *Langmuir* **2003,** *19* (23), 9730-9741.
7.   Yarranton, H. W.; Sztukowski, D. M.; Urrutia, P. Effect of interfacial rheology on model emulsion coalescence: I. Interfacial rheology. *Journal of Colloid and Interface Science* **2007,** *310* (1), 246-252.
8.   Yarranton, H. W.; Urrutia, P.; Sztukowski, D. M. Effect of interfacial rheology on model emulsion coalescence: II. Emulsion coalescence. *Journal of Colloid and Interface Science* **2007,** *310* (1), 253-259.
9.   Buckley, J. S. Asphaltene Deposition. *Energy & Fuels* **2012,** *26* (7), 4086-4090.
10.   Kokal, S. L.; Sayegh, S. G. Asphaltenes: The Cholesterol Of Petroleum. Society of Petroleum Engineers.
11.   Akbarzadeh, K., Hammami, A., Kharrat, A., Zhang, D., Allenson, S., Creek, J., Kabir, S., Jamaluddin, A., Marshall, A., Rodgers, R., Mullins, O., Solbakken, T. Asphaltenes: Problematic but rich in potential. *Oilfield Review* **2007**, 22-43.
12.   Alboudwarej, H.; Akbarzadeh, K.; Beck, J.; Svrcek, W. Y.; Yarranton, H. W. Regular Solution Model for Asphaltene Precipitation from Bitumens and Solvents. *AIChE Journal* **2003,** *49* (11), 2948-2956.
13.   Zougari, M.; Jacobs, S.; Ratulowski, J.; Hammami, A.; Broze, G.; Flannery, M.; Stankiewicz, A.; Karan, K. Novel Organic Solids Deposition and Control Device for Live-Oils: Design and Applications. *Energy & Fuels* **2006,** *20* (4), 1656-1663.
14.   Mullins, O. C. The Asphaltenes. *Annual Review of Analytical Chemistry* **2011,** *4* (1), 393-418.
15.   Wang, J.; Buckley, J. S.; Creek, J. L. Asphaltene Deposition on Metallic Surfaces. *Journal of Dispersion Science and Technology* **2004,** *25* (3), 287-298.
16.   Wang, S.; Liu, J.; Zhang, L.; Masliyah, J.; Xu, Z. Interaction Forces between Asphaltene Surfaces in Organic Solvents. *Langmuir* **2010,** *26* (1), 183-190.

17.   Yang, X.; Kilpatrick, P. Asphaltenes and Waxes Do Not Interact Synergistically and Coprecipitate in Solid Organic Deposits. *Energy & Fuels* **2005,** *19* (4), 1360-1375.

18.   Denoyel, R. In situ methods for studying adsorbed phases at the solid-liquid interface: Microcalorimetry and ellipsometry. *Comptes Rendus - Geoscience* **2002,** *334* (9), 689-702.

19.   Alipour Tabrizy, V.; Denoyel, R.; Hamouda, A. A. Characterization of wettability alteration of calcite, quartz and kaolinite: Surface energy analysis. *Colloids and Surfaces A: Physicochemical and Engineering Aspects* **2011,** *384* (1–3), 98-108.

20.   Denoyel, R. Microcalorimetry and ellipsometry in surfactant adsorption studies. *Colloids and Surfaces A: Physicochemical and Engineering Aspects* **2002,** *205* (1–2), 61-71.

21.   Yarranton, H. W.; Masliyah, J. H. Molar mass distribution and solubility modeling of asphaltenes. *AIChE Journal* **1996,** *42* (12), 3533-3543.

22.   Sjöblom, J.; Aske, N.; Auflem, I. H.; Brandal, Ø.; Havre, T. E.; Sæther, Ø.; Westvik, A.; Johnsen, E. E.; Kallevik, H. Our current understanding of water-in-crude oil emulsions. Recent characterization techniques and high pressure performance. *Advances in Colloid and Interface Science* **2003,** *100-102* (SUPPL.), 399-473.

23.   Sheu, E. Y. Petroleum AsphalteneProperties, Characterization, and Issues. *Energy & Fuels* **2002,** *16* (1), 74-82.

24.   Zahabi, A.; Gray, M. R.; Czarnecki, J.; Dabros, T. Flocculation of Silica Particles from a Model Oil Solution: Effect of Adsorbed Asphaltenes. *Energy & Fuels* **2010,** *24* (6), 3616-3623.

25.   Adams, J. J. Asphaltene adsorption, a literature review. *Energy and Fuels* **2014,** *28* (5), 2831-2856.

26.   Turgman-Cohen, S.; Fischer, D. A.; Kilpatrick, P. K.; Genzer, J. Asphaltene Adsorption onto Self-Assembled Monolayers of Alkyltrichlorosilanes of Varying Chain Length. *ACS Applied Materials & Interfaces* **2009,** *1* (6), 1347-1357.

27.   Dudášová, D.; Simon, S.; Hemmingsen, P. V.; Sjöblom, J. Study of asphaltenes adsorption onto different minerals and clays: Part 1. Experimental adsorption with UV depletion detection. *Colloids and Surfaces A: Physicochemical and Engineering Aspects* **2008,** *317* (1–3), 1-9.

28.   Fritschy, G.; Papirer, E. Interactions between a bitumen, its components and model fillers. *Fuel* **1978,** *57* (11), 701-704.

29.   Tayakout, M.; Ferreira, C.; Espinat, D.; Arribas Picon, S.; Sorbier, L.; Guillaume, D.; Guibard, I. Diffusion of asphaltene molecules through the pore structure of hydroconversion catalysts. *Chemical Engineering Science* **2010,** *65* (5), 1571-1583.

30.   Nassar, N. N.; Hassan, A.; Pereira-Almao, P. Effect of surface acidity and basicity of aluminas on asphaltene adsorption and oxidation. *Journal of Colloid and Interface Science* **2011,** *360* (1), 233-238.

31.   Araújo, R. S.; Azevedo, D. C. S.; Cavalcante Jr, C. L.; Jiménez-López, A.; Rodríguez-Castellón, E. Adsorption of polycyclic aromatic hydrocarbons (PAHs) from isooctane solutions by mesoporous molecular sieves: Influence of the surface acidity. *Microporous and Mesoporous Materials* **2008,** *108* (1–3), 213-222.

32.   Jada, A.; Debih, H. Hydrophobation of Clay Particles by Asphaltenes Adsorption. *Composite Interfaces* **2009,** *16* (2-3), 219-235.

33.   Pernyeszi, T.; Patzkó, Á.; Berkesi, O.; Dékány, I. Asphaltene adsorption on clays and crude oil reservoir rocks. *Colloids and Surfaces A: Physicochemical and Engineering Aspects* **1998,** *137* (1–3), 373-384.

34.   Cosultchi, A.; Cordova, I.; Valenzuela, M. A.; Acosta, D. R.; Bosch, P.; Lara, V. H. Adsorption of Crude Oil on Na+-Montmorillonite. *Energy & Fuels* **2005,** *19* (4), 1417-1424.

35.   Dudášová, D.; Silset, A.; Sjöblom, J. Quartz Crystal Microbalance Monitoring of Asphaltene Adsorption/Deposition. *Journal of Dispersion Science and Technology* **2008,** *29* (1), 139-146.

36.   Clementz, D. Interaction of Petroleum Heavy ends with Montmorillonite. *Clays and Clay Minerals* **1976,** *24*, 312-319.

37.   Tombácz, E.; Szekeres, M. Surface charge heterogeneity of kaolinite in aqueous suspension in comparison with montmorillonite. *Applied Clay Science* **2006,** *34* (1–4), 105-124.

38.   Sjöblom, J.; Simon, S.; Xu, Z. Model molecules mimicking asphaltenes. *Advances in Colloid and Interface Science* **2015,** *218*, 1-16.

39.   Nalwaya, V.; Tantayakom, V.; Piumsomboon, P.; Fogler, S. Studies on Asphaltenes through Analysis of Polar Fractions. *Industrial & Engineering Chemistry Research* **1999,** *38* (3), 964-972.

40.   Yen, T. F.; Erdman, J. G.; Pollack, S. S. Investigation of the Structure of Petroleum Asphaltenes by X-Ray Diffraction. *Analytical Chemistry* **1961,** *33* (11), 1587-1594.

41.   Espinat, D. Application of Light, X-ray and Neutron diffusion Techniques to the study of colloidal systems. *Rev. Inst. Fr. Pet* **1991,** *45*, 775-820.

42.   Groenzin, H.; Mullins, O. C. Asphaltene Molecular Size and Structure. *The Journal of Physical Chemistry A* **1999,** *103* (50), 11237-11245.

43.   Groenzin, H.; Mullins, O. C.; Eser, S.; Mathews, J.; Yang, M.-G.; Jones, D. Molecular Size of Asphaltene Solubility Fractions. *Energy & Fuels* **2003,** *17* (2), 498-503.

44.   Akbarzadeh, K.; Bressler, D. C.; Wang, J.; Gawrys, K. L.; Gray, M. R.; Kilpatrick, P. K.; Yarranton, H. W. Association Behavior of Pyrene Compounds as Models for Asphaltenes. *Energy & Fuels* **2005,** *19* (4), 1268-1271.

45.   Tan, X.; Fenniri, H.; Gray, M. R. Pyrene Derivatives of 2,2′-Bipyridine as Models for Asphaltenes: Synthesis, Characterization, and Supramolecular Organization. *Energy & Fuels* **2008,** *22* (2), 715-720.

46.   Alshareef, A. H.; Scherer, A.; Tan, X.; Azyat, K.; Stryker, J. M.; Tykwinski, R. R.; Gray, M. R. Effect of Chemical Structure on the Cracking and Coking of Archipelago Model Compounds Representative of Asphaltenes. *Energy & Fuels* **2012,** *26* (3), 1828-1843.

47.   Kuznicki, T.; Masliyah, J. H.; Bhattacharjee, S. Molecular Dynamics Study of Model Molecules Resembling Asphaltene-Like Structures in Aqueous Organic Solvent Systems. *Energy & Fuels* **2008,** *22* (4), 2379-2389.

48.   Kuznicki, T.; Masliyah, J. H.; Bhattacharjee, S. Aggregation and Partitioning of Model Asphaltenes at Toluene−Water Interfaces: Molecular Dynamics Simulations. *Energy & Fuels* **2009,** *23* (10), 5027-5035.

49.   Nordgård, E. L.; Sørland, G.; Sjöblom, J. Behavior of asphaltene model compounds at W/O interfaces. *Langmuir* **2010,** *26* (4), 2352-2360.

50.   Nordgård, E. L.; Landsem, E.; Sjöblom, J. Langmuir Films of Asphaltene Model Compounds and Their Fluorescent Properties. *Langmuir* **2008,** *24* (16), 8742-8751.

51.   Nordgård, E. L.; Sjoblom, J. Model compounds for asphaltenes and C80 isoprenoid tetraacids. Part I: Synthesis and interfacial activities. *Journal of Dispersion Science and Technology* **2008,** *29* (8), 1114-1122.

52.   Bi, J.; Yang, F.; Harbottle, D.; Pensini, E.; Tchoukov, P.; Simon, S.; Sjöblom, J.; Dabros, T.; Czarnecki, J.; Liu, Q.; Xu, Z. Interfacial Layer Properties of a Polyaromatic Compound and its Role in Stabilizing Water-in-Oil Emulsions. *Langmuir* **2015,** *31* (38), 10382-10391.

53.   Wei, D.; Orlandi, E.; Barriet, M.; Simon, S.; Sjöblom, J. Aggregation of tetrameric acid in xylene and its interaction with asphaltenes by isothermal titration calorimetry. *Journal of Thermal Analysis and Calorimetry* **2015,** *122* (1), 463-471.

54.   Holman, M. W.; Liu, R.; Adams, D. M. Single-Molecule Spectroscopy of Interfacial Electron Transfer. *Journal of the American Chemical Society* **2003**, *125* (41), 12649-12654.

55.   Nasir, S. M., N.; Augie, N. M. Geochemical Study of Crude Oil Samples to Evaluate Extent and Effect of Secondary Alteration Process (i.e. Biodegradation). *International Journal of Scientific and Research Publications (IJSRP)* **2014,** *4* (10), 12.

56.   Simon, S.; Sjöblom, J.; Wei, D. Interfacial and Emulsion Stabilizing Properties of Indigenous Acidic and Esterified Asphaltenes. *Journal of Dispersion Science and Technology* **2016**, DOI: 10.1080/01932691.2015.1135808.

57.   Simon, S.; Reisen, C.; Bersås, A.; Sjöblom, J. Reaction between tetrameric acids and Ca 2+ in oil/water system. *Industrial and Engineering Chemistry Research* **2012,** *51* (16), 5669-5676.

58.   Sauerbrey, G. Verwendung von Schwingquarzen zur Wägung dünner Schichten und zur Mikrowägung. *Z. Physik* **1959,** *155* (2), 206-222.

59.   Rodahl, M., Höök, F., Krozer, A., Brzezinski, P., Kasemo, B. Quartz crystal microbalance setup for frequency and Q-factor measurements in gaseous and liquid environments. *Review of Scientific Instruments* **1995,** *66*, 3924-3930.

60.   Denoyel, R.; Glez, J. C.; Trens, P. Grafting γ-aminopropyl triethoxysilane onto silica: consequence on polyacrylic acid adsorption. *Colloids and Surfaces A: Physicochemical and Engineering Aspects* **2002,** *197* (1–3), 213-223.

61.   Trens, P.; Denoyel, R. Conformation of poly(ethylene glycol) polymers at the silica/water interface: a microcalorimetric study. *Langmuir* **1993,** *9* (2), 519-522.

62.   Goncalves, S.; Castillo, J.; Fernández, A.; Hung, J. Absorbance and fluorescence spectroscopy on the aggregation behavior of asphaltene–toluene solutions. *Fuel* **2004,** *83* (13), 1823-1828.

63.   Turgman-Cohen, S.; Smith, M. B.; Fischer, D. A.; Kilpatrick, P. K.; Genzer, J. Asphaltene Adsorption onto Self-Assembled Monolayers of Mixed Aromatic and Aliphatic Trichlorosilanes. *Langmuir* **2009,** *25* (11), 6260-6269.

64.   Verruto, V. J.; Le, R. K.; Kilpatrick, P. K. Adsorption and Molecular Rearrangement of Amphoteric Species at Oil−Water Interfaces. *The Journal of Physical Chemistry B* **2009,** *113* (42), 13788-13799.

65.   Atkins, P., De Paula, J. *Atkins' Physical Chemistry*; 8th ed.; Oxford University Press2006.

66.   Sinnokrot, M. O.; Valeev, E. F.; Sherrill, C. D. Estimates of the Ab Initio Limit for π−π Interactions: The Benzene Dimer. *Journal of the American Chemical Society* **2002,** *124* (36), 10887-10893.

67.   Simon, S.; Wei, D.; Barriet, M.; Sjöblom, J. An ITC and NMR study of interaction and complexation of asphaltene model compounds in apolar solvent I: Self-association pattern. *Colloids and Surfaces A: Physicochemical and Engineering Aspects* **2016,** *494*, 108-115.

68.   Nenningsland, A. L.; Simon, S.; Sjöblom, J. Surface properties of basic components extracted from petroleum crude oil. *Energy and Fuels* **2010,** *24* (12), 6501-6505.

69.   Sztukowski, D. M.; Jafari, M.; Alboudwarej, H.; Yarranton, H. W. Asphaltene self-association and water-in-hydrocarbon emulsions. *Journal of Colloid and Interface Science* **2003,** *265* (1), 179-186.

70.   Alboudwarej, H.; Pole, D.; Svrcek, W. Y.; Yarranton, H. W. Adsorption of Asphaltenes on Metals. *Industrial & Engineering Chemistry Research* **2005,** *44* (15), 5585-5592.

71.   Kokal, S.; Tang, T.; Schramm, L.; Sayegh, S. Electrokinetic and adsorption properties of asphaltenes. *Colloids and Surfaces A: Physicochemical and Engineering Aspects* **1995,** *94* (2–3), 253-265.

72.   González, G.; Middea, A. The properties of the calcite—solution interface in the presence of adsorbed resins or asphaltenes. *Colloids and Surfaces* **1988,** *33*, 217-229.

73.   Wright, E. H. M.; Pratt, N. C. Solid/solution interface equilibria for aromatic molecules adsorbed from non-aromatic media. Part 2.-Aromatic carboxylic acids. *Journal of the Chemical Society, Faraday Transactions 1: Physical Chemistry in Condensed Phases* **1974,** *70* (0), 1461-1471.

74.   Poteau, S.; Argillier, J.-F.; Langevin, D.; Pincet, F.; Perez, E. Influence of pH on Stability and Dynamic Properties of Asphaltenes and Other Amphiphilic Molecules at the Oil−Water Interface. *Energy & Fuels* **2005,** *19* (4), 1337-1341.

75.   Strassne, J. Effect of pH on interfacial films and stability of crude oil-water emulsions. *Journal of Petroleum Technology* **1968,** *20*, 303-312.

76.   Xie, K.; Karan, K. Kinetics and Thermodynamics of Asphaltene Adsorption on Metal Surfaces: A Preliminary Study. *Energy & Fuels* **2005,** *19* (4), 1252-1260.

77.   Sirota, E. B. Swelling of Asphaltenes. *Petroleum Science and Technology* **1998,** *16* (3-4), 415-431.

78.   Hannisdal, A.; Orr, R.; Sjöblom, J. Viscoelastic properties of crude oil components at oil-water interfaces. 1. The effect of dilution. *Journal of Dispersion Science and Technology* **2007,** *28* (1), 81-93.
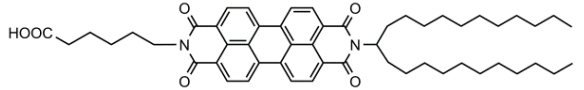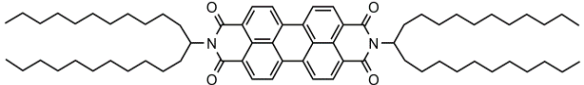
Table 1: Properties of the heavy crude oil sample used in this work for asphaltene extraction. (*): determined by Karl-Fisher titration. (**): the SARA composition determination method by HPLC is described by Hannisdal et al[78].

Density @ 15°C	TAN (mg.g^{-1})	Water content (wt. %) (*)	SARA analysis (**)			
			Saturates (wt. %)	Aromatics (wt. %)	Resins (wt. %)	Asphaltenes, hexane insoluble (wt. %)
0.939	2.15	0.11	37	44	16	2.5

Table 2. Elemental composition of asphaltenes recovered from the heavy crude oil used in this work.

	% C	% H	% N	% O	% S	C/H atomic ratio
Asphaltenes	86.1	8.28	1.29	1.97	2.10	0.867

Table 3. General aspects of the model compounds used in this study.

Compound	Molar mass g/mol	Structure
C5PeC11	827.12	
BisAC11	1035.60	

Table 4. Overview of the properties of the surfaces used in this work and calculated interfacial quantities.

Surface	Specific Surface Area (m²/g)^a	Contact Angle^b	C5PeC11 Γ_p (mg/m²)^c	C5PeC11 m (kJm²/mol²) Eq. (4)	C5PeC11 ΔH_z(kJ/mol) Eq. (4)	Asphaltenes Γ_p (mg/m²)^c	Asphaltenes m (kJm²/mol²) Eq. (4)	Asphaltenes ΔH_z (kJ/mol) Eq. (4)
Silica	203 ± 7	5.5 ± 0.4°	0.91	7 x10^6	-34.9	1.32	-9 x10^6	-8.9
CaCO$_3$	19 ± 1	21.8 ± 1.9°	2.94	6 x10^6	-23.5	1.54	-23 x10^6	-18.7
Stainless Steel	4.1 ± 0.1	56.4 ± 1.1°	3.96	4 x10^6	-7.7	1.94	-12 x10^6	-4.6

^{a}. Determined via gas adsorption and fitted to the BET equation.

^{b}. Determined on coated-quartz crystals.

^{c}. Average adsorbed amount in the plateau region of figure 1 and figure 2.
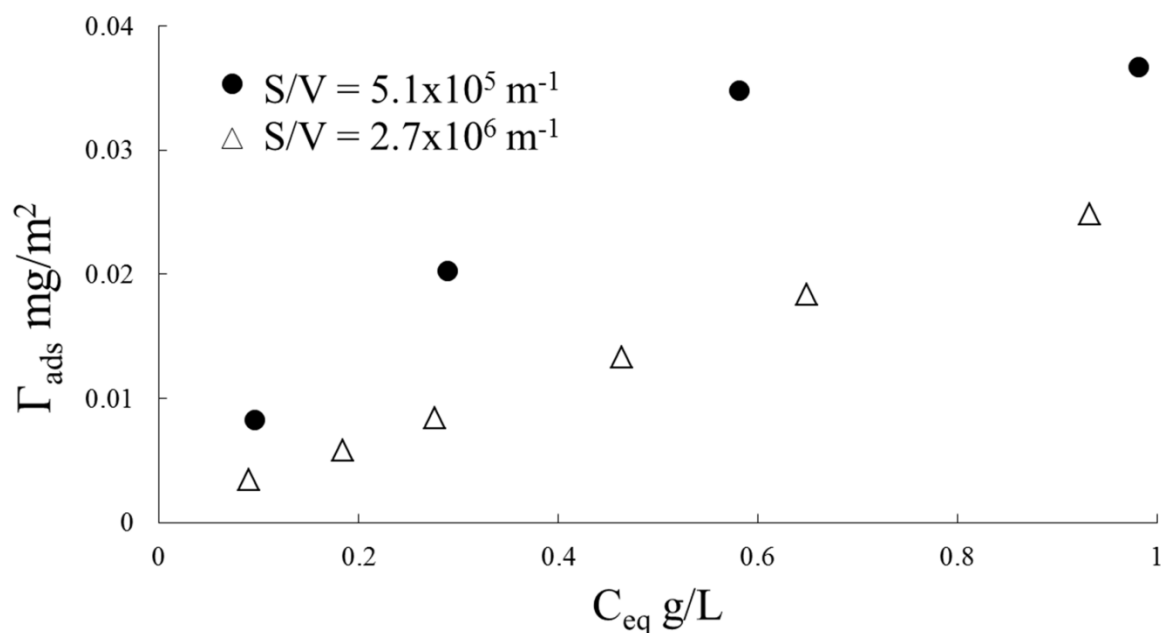
Figure 1. Adsorption of the model compound C5PeC11 onto silica, $CaCO_3$ (calcite) and stainless steel particles. The equilibrium and initial concentrations were measured via HPLC. The lines are visual aides.
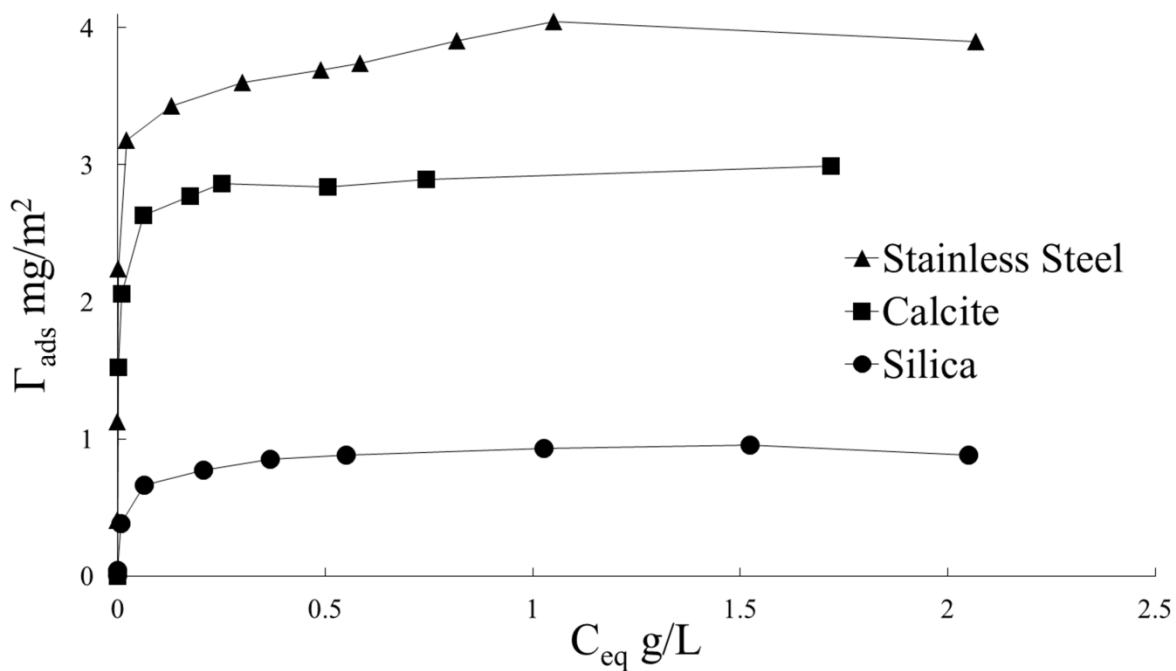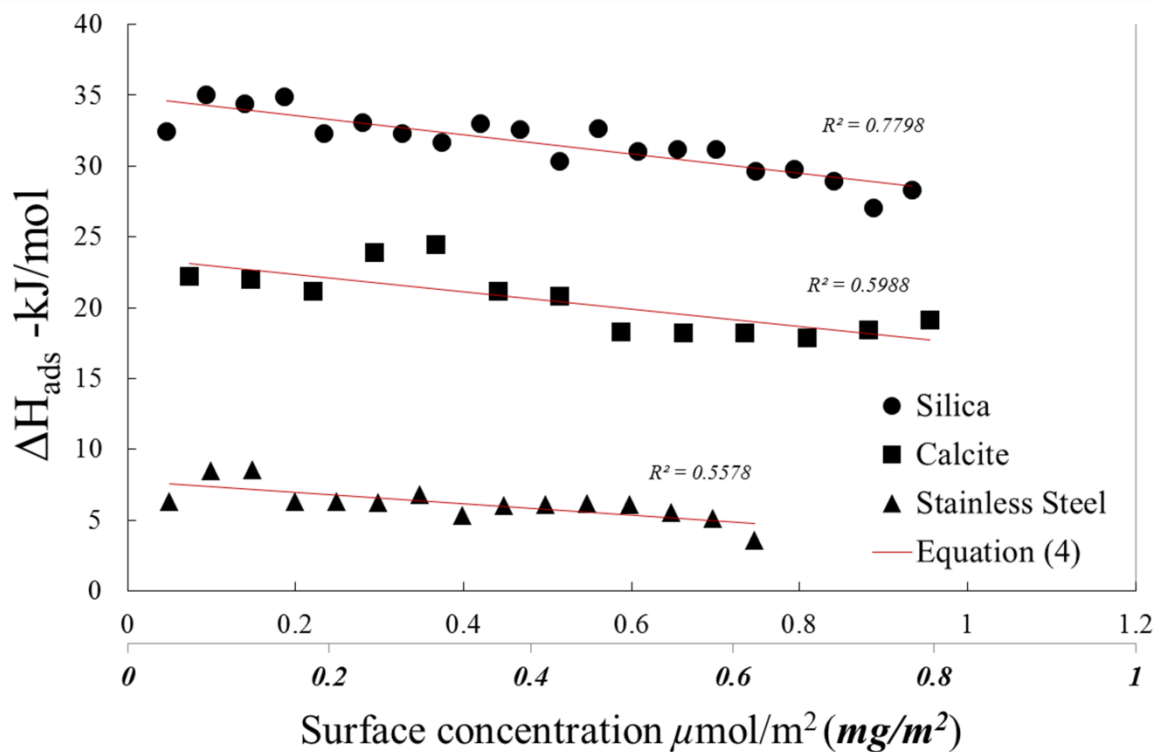

Figure 2. Adsorption of C_6-asphaltenes onto silica, $CaCO_3$ (calcite) and stainless steel particles. The equilibrium and initial concentrations were measured via UV-spectrophotometry. The lines are visual aides.
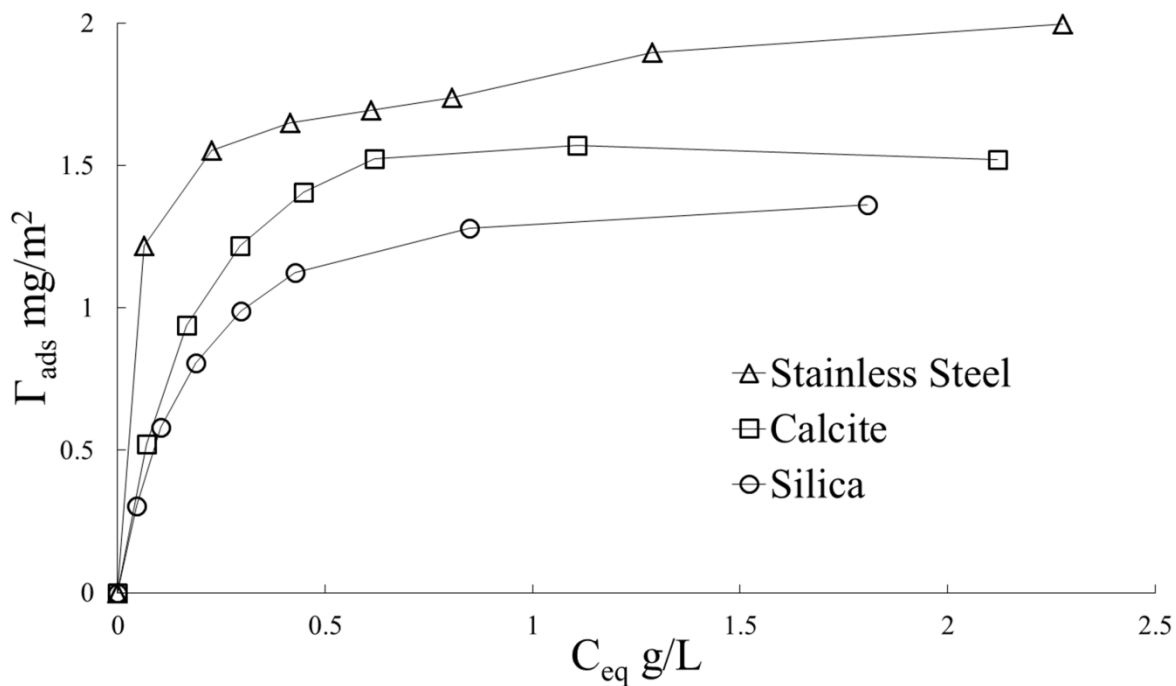
Figure 3. Adsorption of the model compound BisAC11 onto silica. The equilibrium and initial concentrations were measured via UV-spectrophotometry. Two surface-to-volume of oil ratios (S/V in m^{-1}) are shown.


Figure 4. Differential enthalpy of adsorption as a function of the surface concentration for the model compound C5PeC11 onto silica, calcite and stainless steel. Solid lines represent the fit to Equation (4).

Figure 5. Differential enthalpy of adsorption as a function of the surface concentration for C_6-asphaltenes onto silica, calcite and stainless steel. Solid lines represent the fit to Equation (4).
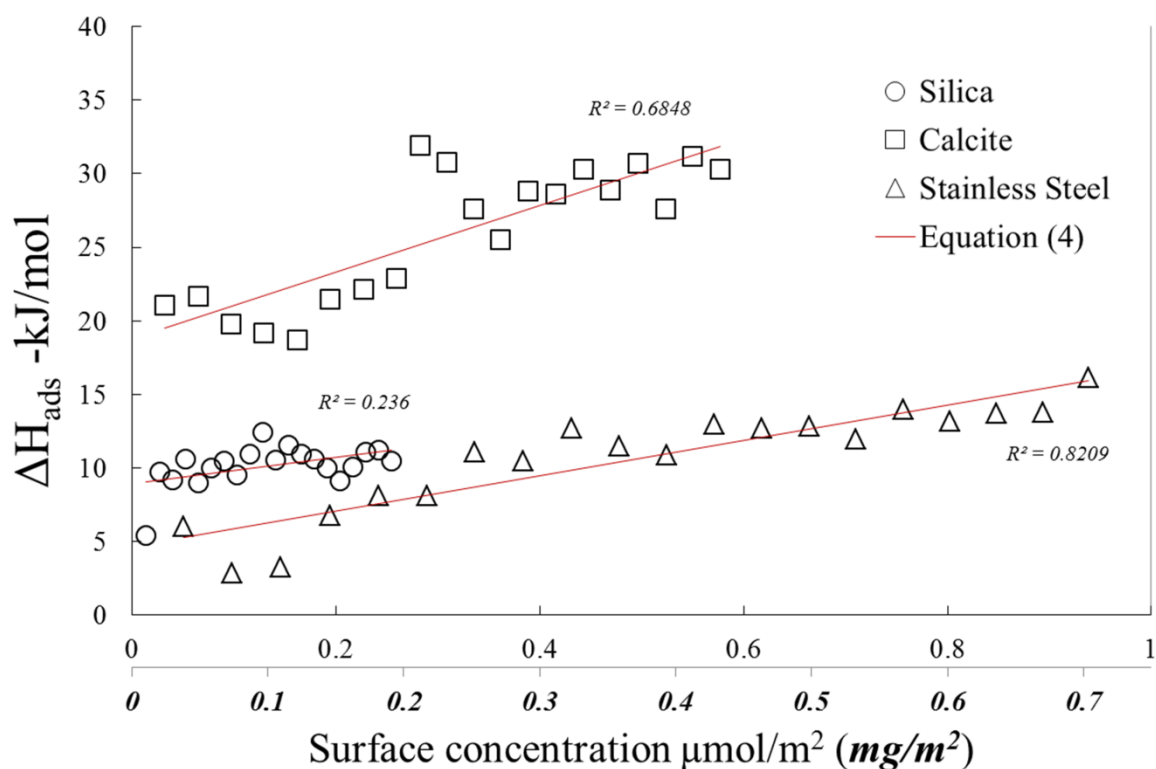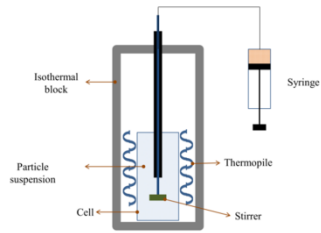

Figure 6. Asphaltene (Asph) and esterified-asphaltene (E-Asph) isotherms measured via the depletion method (DM) and quartz crystal microbalance (QCM) experiments onto two surfaces: stainless steel (open triangles) and silica (open circles). The lines are visual aides.
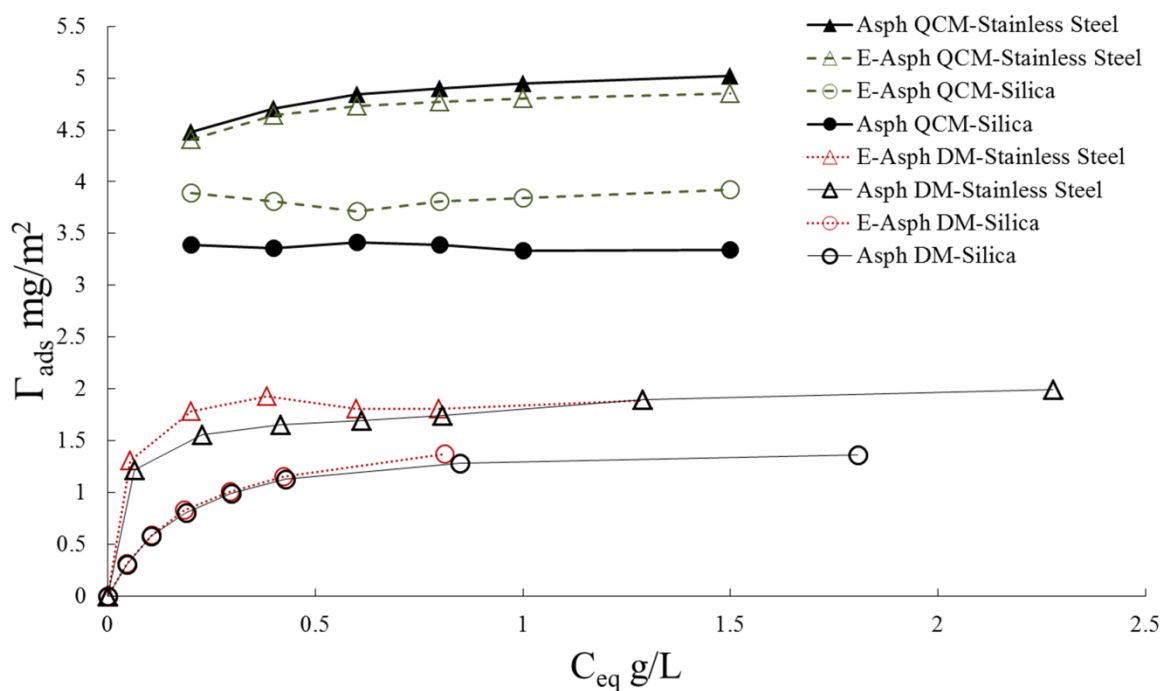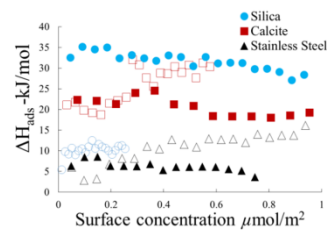
Table of contents graphic

Microcalorimetry of
polyaromatic molecules

Enthalpy of
Adsorption

Determination of the
driving force and
type of interaction at
the liquid/solid
surface